



HAL
open science

Method development for PPB culture screening, pigment analysis with UPLC-UV-HRMS vs. spectrophotometric methods, and spectral decomposition-based analysis

Maria Grassino, Damien J Batstone, Ken W L Yong, Gabriel Capson-Tojo,
Tim Hülsen

► To cite this version:

Maria Grassino, Damien J Batstone, Ken W L Yong, Gabriel Capson-Tojo, Tim Hülsen. Method development for PPB culture screening, pigment analysis with UPLC-UV-HRMS vs. spectrophotometric methods, and spectral decomposition-based analysis. *Talanta*, 2022, 246, 10.1016/j.talanta.2022.123490 . hal-03777893

HAL Id: hal-03777893

<https://hal.inrae.fr/hal-03777893>

Submitted on 13 Aug 2023

HAL is a multi-disciplinary open access archive for the deposit and dissemination of scientific research documents, whether they are published or not. The documents may come from teaching and research institutions in France or abroad, or from public or private research centers.

L'archive ouverte pluridisciplinaire **HAL**, est destinée au dépôt et à la diffusion de documents scientifiques de niveau recherche, publiés ou non, émanant des établissements d'enseignement et de recherche français ou étrangers, des laboratoires publics ou privés.

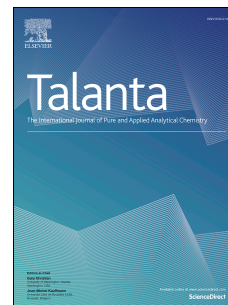


Distributed under a Creative Commons Attribution - NonCommercial - NoDerivatives 4.0
International License

Journal Pre-proof

Method development for PPB culture screening, pigment analysis with UPLC-UV-HRMS vs. spectrophotometric methods, and spectral decomposition-based analysis

Maria Grassino, Damien J. Batstone, Ken W.L. Yong, Gabriel Capson-Tojo, Tim Hülsen



PII: S0039-9140(22)00286-7

DOI: <https://doi.org/10.1016/j.talanta.2022.123490>

Reference: TAL 123490

To appear in: *Talanta*

Received Date: 1 February 2022

Revised Date: 12 April 2022

Accepted Date: 15 April 2022

Please cite this article as: M. Grassino, D.J. Batstone, K.W.L. Yong, G. Capson-Tojo, T. Hülsen, Method development for PPB culture screening, pigment analysis with UPLC-UV-HRMS vs. spectrophotometric methods, and spectral decomposition-based analysis, *Talanta* (2022), doi: <https://doi.org/10.1016/j.talanta.2022.123490>.

This is a PDF file of an article that has undergone enhancements after acceptance, such as the addition of a cover page and metadata, and formatting for readability, but it is not yet the definitive version of record. This version will undergo additional copyediting, typesetting and review before it is published in its final form, but we are providing this version to give early visibility of the article. Please note that, during the production process, errors may be discovered which could affect the content, and all legal disclaimers that apply to the journal pertain.

© 2022 Published by Elsevier B.V.

Maria Grassino: Conceptualization, Methodology, Software, Validation, Formal analysis, Data, Curation Investigation, Writing - Original Draft, Visualization, Project administration

Damien J. Batstone: Conceptualization, Methodology, Software, Validation, Formal analysis, Writing - Review & Editing Resources, Supervision, Funding acquisition

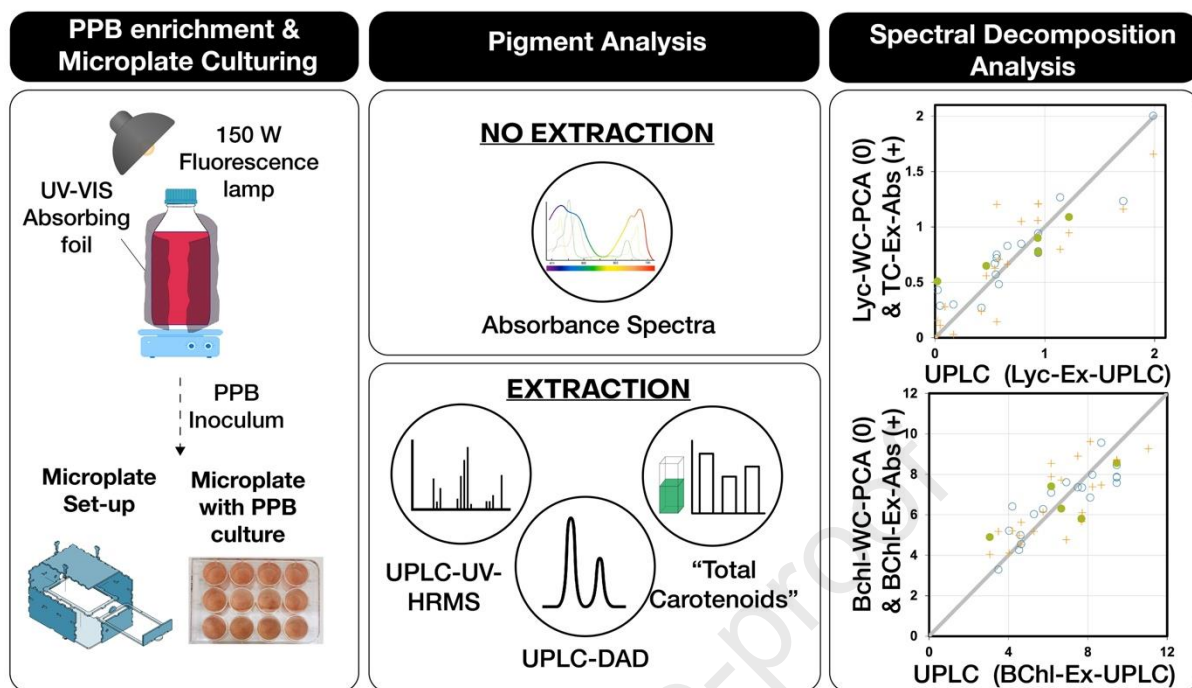
Ken W.L. Yong: Methodology, Writing - Review & Editing Resources, Supervision

Gabriel Capson-Tojo: Methodology, Writing - Review & Editing Resources

Tim Hülsen: Conceptualization, Methodology, Validation, Resources, Writing - Review & Editing, Supervision, Project administration, Funding acquisition

Journal Pre-proof

Graphical abstract



1 **Method development for PPB culture screening, pigment analysis with UPLC-UV-HRMS**
2 **vs. spectrophotometric methods, and spectral decomposition-based analysis**

3 Maria Grassino ^a, Damien J. Batstone ^a, Ken W.L. Yong ^c, Gabriel Capson-Tojo ^{a,b}, Tim
4 Hülsen^a

5

6 ^a Australian Centre for Water and Environmental Biotechnology, The University of
7 Queensland, Brisbane, QLD 4072, Australia

8 ^b CRETUS Institute, Department of Chemical Engineering, Universidade de Santiago de
9 Compostela, 15782 Santiago de Compostela, Galicia, Spain

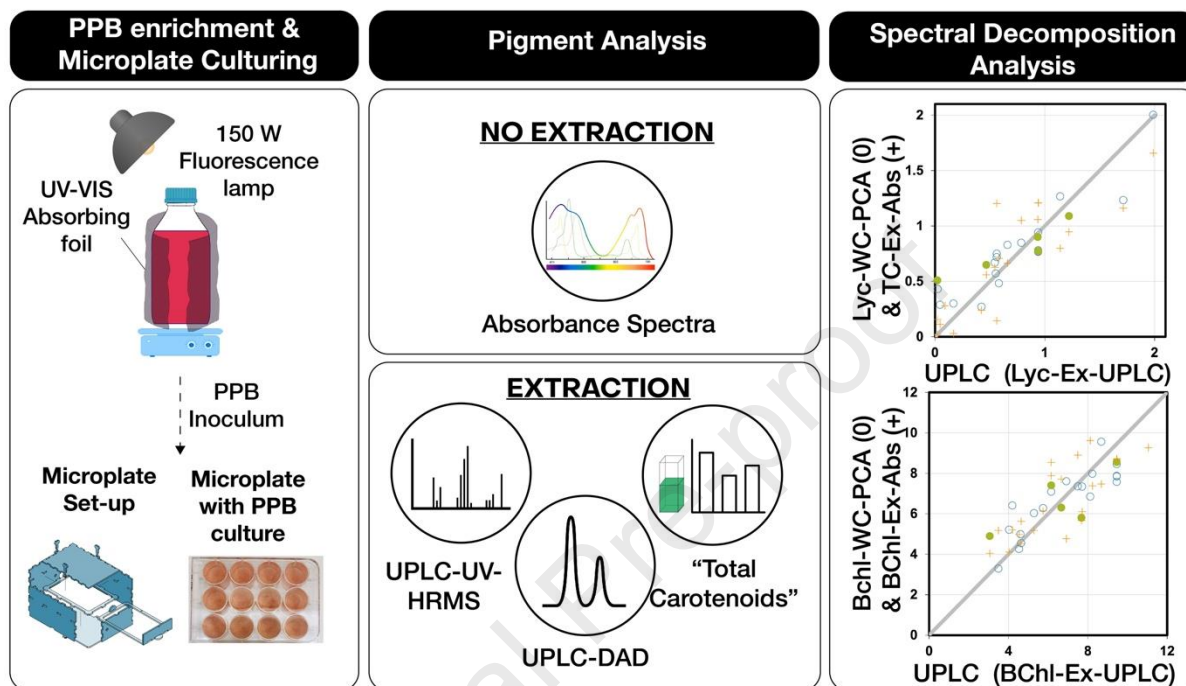
10 ^c Biosecurity Queensland, Department of Agriculture and Fisheries, Queensland Government,
11 Health and Food Sciences Precinct, Coopers Plains, QLD 4108, Australia

12 **Abstract**

13 PPB carotenoids are usually measured through spectrophotometric analysis, measuring total
14 carotenoids (TCs) which has low accuracy and cannot identify individual carotenoids or
15 isomers. Here, we developed an ultra-performance liquid chromatography method with
16 ultraviolet and high-resolution mass spectrometry detection (UPLC-UV-HRMS) to quantify
17 neurosporene, lycopene, and bacteriochlorophyll a contents in PPB cultures. The method
18 exhibited satisfactory recoveries for individual pigments (between 82.1% and 99.5%) and was
19 applied to a range of mixed PPB cultures. The use of a C₃₀ column also enabled the detection
20 of three different isomers of lycopene. In addition, a method for anaerobic photoheterotrophic
21 PPB cultivation to acquire live-cell spectrophotometric information was developed and tested
22 by modifying a standard microbial culture microplate system. A rapid, and relatively low effort
23 principal component analysis (PCA) based decomposition of the whole-cell spectra for
24 pigment analysis in the microplates was also developed. Analysing whole-cell spectra via PCA
25 allowed more accurate prediction of individual pigments compared to absorption methods, and

26 can be done non-destructively, during live-cell growth, but requires calibration for new media
 27 and microbial matrices.

28 Graphical abstract



29

30 Keywords

31 Purple phototrophic bacteria; Pigments; Carotenoid; Lycopene; Bacteriochlorophyll

32

33 Highlights

- 34 • A UPLC-UV-HRMS method to detect and quantify PPB pigments was developed
- 35 • A C₃₀ column enabled detection and quantification of two lycopene isomers
- 36 • A microplate method for photoheterotrophic PPB cultivation was developed
- 37 • Pigment contents can be determined by PCA on the whole-cell spectra

38

39 Acronyms and Symbols

40	APCI	Atmospheric pressure chemical ionization
41	ASV	Amplicon sequencing variants
42	BChl	Bacteriochlorophyll
43	BHT	Butylated hydroxytoluene
44	COD	Chemical oxygen demand
45	DNA	Deoxyribonucleic acid
46	$E_{\bar{x}}$	Estimated error at 95% confidence level
47	HPLC	High-performance liquid chromatography
48	HPLC-MS	High-performance liquid chromatography-mass spectrometry
49	HRMS	High-resolution mass spectrometry
50	IR	Infrared
51	LC	Liquid chromatography
52	LED	Light-emitting diode
53	LHC	Light harvesting complexes
54	MeOH	Methanol
55	MP	Mobile phase
56	MTBE	Methyl-tert-butyl ether
57	OD	Optical density
58	PCA	Principal component analysis
59	PC	Principal component
60	pCOD	Particulate COD

61	PCG	Photosynthetic gene cluster
62	PPB	Purple phototrophic bacteria
63	R^2	Coefficient of determination
64	RNA	Ribonucleic acid
65	rRNA	Ribosomal ribonucleic acid
66	RSD	Relative standard deviation
67	SCOD	Soluble chemical oxygen demand
68	SCP	Single-cell protein
69	S_{xi}	Standard deviation
70	TC	Total carotenoids
71	TCOD	Total chemical oxygen demand
72	UPLC	Ultra-high performance liquid chromatography
73	UV	Ultraviolet
74	VIS	Visible
75	\bar{X}	Average value

76

77 **1 Introduction**

78 The production and extraction of natural carotenoids from microbial cultures is an area of
79 research receiving increasing attention. To date, around 600 naturally occurring carotenoids
80 with various functional properties have been identified [1, 2]. Natural carotenoids are
81 significantly superior to synthetic compounds in terms of beneficial properties [3] but also incur
82 significantly higher production costs compared with synthetic products. This is mainly due to
83 harvesting and extraction, which account for up to 90% of the production costs [4, 5]. For

84 example, the β -carotene extraction costs from *Dunaliella salina* are 10.38 ± 0.99 USD
85 kg^{-1} when using organic solvents and 7.7 ± 0.83 USD kg^{-1} with supercritical carbon dioxide
86 extraction [6]. As an alternative, carotenoids contained in pure or mixed microbial cultures can
87 be used as whole-cell products (e.g. as carotenoid-rich single-cell protein (SCP)) [7]. In this
88 context, purple phototrophic bacteria (PPB) are a group of anoxygenic phototrophic
89 microorganisms that generate bacteriochlorophyll (BChl) and carotenoids during
90 photoheterotrophic growth under anaerobic-illuminated conditions. Without dedicated content
91 manipulation, carotenoid contents of PPB biomass were reported in the range of 1.0 to >12
92 $\text{mg}\cdot\text{VS}^{-1}$ [8], but can reach $>1.7 \text{ g}_{\text{carotenoids}}\cdot\text{L}^{-1}$ in concentrated biofilms [9].

93 The most commonly used method to quantify the carotenoid content in PPB biomass has been
94 solvent (acetone/methanol) extraction combined with ultraviolet-visible (UV–VIS) absorption
95 detection, measuring the TC content. However, the accuracy of this quantification method for
96 PPB with an unknown carotenoid composition is questionable because the extinction
97 coefficients are unknown, especially for carotenoid mixtures. However, PPB samples normally
98 consist of an unknown, complex matrix of more than one carotenoid, which differs depending
99 on the species, growth stage, and growth conditions [10].

100 Separation through liquid chromatography on pigment extract is required to determine the
101 carotenoid profile. The use of analytical standards in High Performance Liquid
102 Chromatography (HPLC) studies on PBB carotenoids is rare and the identification is usually
103 based on the retention time and UV spectra [11-13]. The main reason for this is that carotenoid
104 standards are expensive and notoriously unstable due to UV light, temperature, and oxygen
105 enhanced degradation [14, 15]. A further limitation of PPB studies using HPLC is the
106 widespread use of C_{18} columns, which are not able to resolve geometrical isomers and
107 inefficiently resolve positional isomers [11-13]. Yet, in nature carotenoids exist in different
108 isomer forms (the main difference with synthetic products), which results in different
109 bioavailability and effects when ingested with the diet [16, 17]. A non-encapped reverse
110 phase (RP)-HPLC column with triacontyl (C_{30}) can be used to maximise chromatographic

111 resolution and selectivity of carotenoids and their isomers [18, 19]. High-performance and
112 ultra-performance liquid chromatography coupled with mass spectrometry (HPLC-MS, UPLC-
113 MS) and using suitable analytical standards are the most effective tools for the detection and
114 quantification of PPB carotenoids [20, 21]. However, methods based on these techniques are
115 expensive, somewhat slow, and cannot be used *in* or *ex-situ* during growth experiments (*e.g.*,
116 to determine maximum carotenoid extent), since an extraction and analysis process is
117 required.

118 This study aims to address pigment identification and quantification in PPB by using ultra-
119 performance liquid chromatography with UV and high-resolution mass spectrometry detection
120 (UPLC-UV-HRMS), to analyse and quantify neurosporene, lycopene, and BChl a. We also
121 developed a modified high-throughput microplate culture protocol to enable anaerobic
122 photoheterotrophic PPB cultivation with live-cell absorption spectrum collection (in a plate
123 reader). Whole (live) cell, as well as extract spectra are decomposed by principal component
124 analysis, and the principal components analysed for the ability to predict UPLC extract
125 analysis of lycopene and BChl. This provides a non-destructive, rapid pigment analysis
126 method for PPB cultures, also assessing the relevance of spectrophotometric methods for
127 pigment quantification.

128

129 **2 Material and methods**

130 **2.1 Inoculum, media composition, and enrichment procedure**

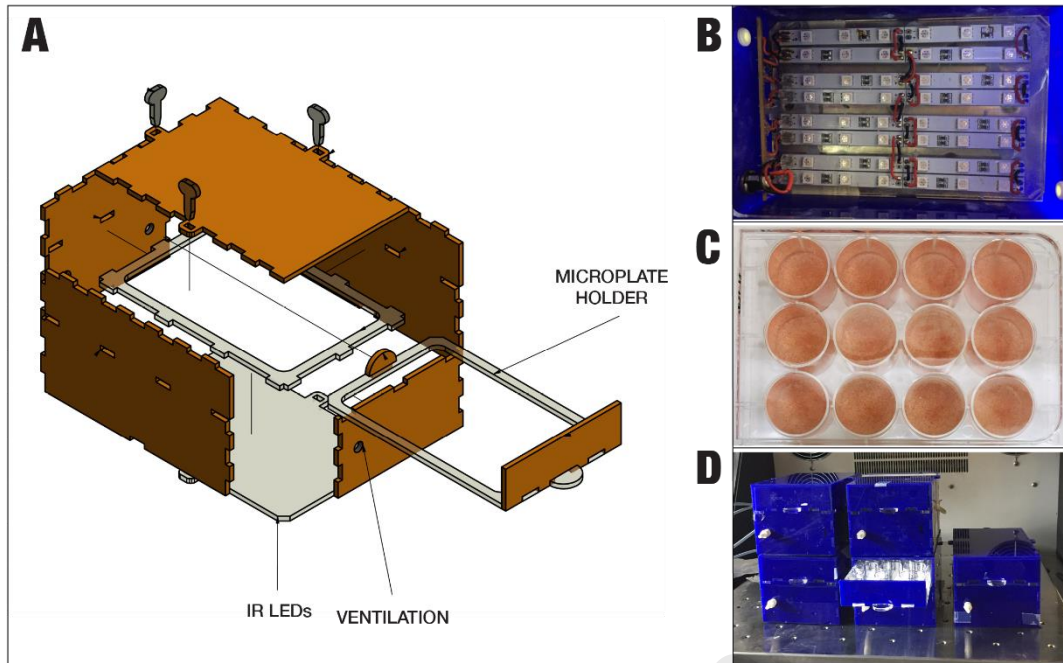
131 Six enrichments cultures were started using inoculum sources from sediments harvested from
132 the Brisbane River (Tuckean Broadwater, -28.987226, 153.407759) and Ballina Mangrove
133 Habitat (28.84159418, 153.5703618) in New South Wales (Australia), as well as samples of
134 poultry and domestic wastewaters (Brisbane, Australia). NaCl was added to the enrichments
135 in different concentrations to increase the salinity to 30 and 70 mS·cm⁻¹, aiming to select for
136 halotolerant and halophilic PPB genera [22] and thus increase the overall microbial diversity,

137 which would allow to test and validate the proposed pigment quantification method (see
138 Section 2.4) under different scenarios. The resulting enrichments were designated as E1-E6,
139 corresponding to sediments from Tuckean Broadwater and sea salt addition of $30 \text{ mS}\cdot\text{cm}^{-1}$
140 (E1), Ballina Mangrove Habitat, and salt addition of $30 \text{ mS}\cdot\text{cm}^{-1}$ (E2) and $70 \text{ mS}\cdot\text{cm}^{-1}$ (E3),
141 Brisbane River (E4), poultry processing wastewater (E5) and domestic wastewater (E6).

142 For these enrichments, six reactors (Schott bottles with a working volume of 500 mL) were
143 filled with 400mL of the different environmental sources and inoculated with $500 \text{ mg COD}\cdot\text{L}^{-1}$
144 of acetic acid, and the different NaCl concentrations for 10 days, until a visible colour shift
145 developed. Subsequently, the enrichments were maintained and fed every 5 days with fresh,
146 modified Ormerod medium [23], containing $500 \text{ mg COD}\cdot\text{L}^{-1}$ of acetic acid and $405 \text{ mg}\cdot\text{L}^{-1}$ of
147 NH_4Cl . The headspace of the bottles was flushed with N_2 to remove oxygen traces.
148 Afterwards, the pH was adjusted to 6.8 (2M NaOH) and the bottles were closed and covered
149 with UV-VIS light absorbing foil (ND 1.2 299, Lee Filter, Transformation Tubes) to exclude
150 wavelengths lower than 790 nm. The bottles were incubated at ambient temperature (23-25
151 °C) mixed with magnetic stirrers at 150 rpm, and they were illuminated from the side with a
152 150 W fluorescence lamp (Nelson Clamp Flood Light), resulting in an incident intensity of ~ 90
153 $\text{W}\cdot\text{m}^{-2}$.

154 **2.2 Microplate set-up and tests for in vivo and extracted spectral data acquisition**

155 A series of custom-made stackable, non-transparent acrylic boxes (139 x 92 x 80 mm) were
156 used to fit 12-well, transparent polystyrene microplates in an integrated, removable plate
157 holder. This system allowed to minimise external light effects, avoid light attenuation issues
158 and enable easy access for sampling (Figure 1).



159

160 **Figure 1.** (A) Schematic of the acrylic box, (B) LED strips attached on the bottom of the
 161 boxes, (C) an example of PPB cultures grown in the set-up, and (D) picture of the set up
 162 showing a microplate.

163 Microplates were clear flat-bottom polystyrene plates with 12 wells, each with a volume of 6.9
 164 mL (Costar®, Bio-Strategy Pty Limited, Tullamarine, Australia). The plate material did not
 165 attenuate the light based on measurements (data not shown). Each box encased 4 rigid strips
 166 containing 12 infrared (IR; 850 nm/940 nm) light-emitting diodes (LEDs, LEDLightsWorld LTD)
 167 placed at the bottom, at a distance of 50 mm from the microplate holder, to ensure optimal
 168 light distribution (Figure 1B) (Note, NIR LED could be exchanged with other light sources to
 169 study the effects). A dimmer enabled light intensity changes between 0 and $40 \text{ W} \cdot \text{m}^{-2}$ for each
 170 set-up. The light intensity was measured with a StellarNet BLUE-Wave Spectrometer
 171 (StellarNet Inc, Florida, USA). Specifically, the emitted irradiances were measured at 12
 172 coordinates, corresponding to each of the microplate's wells. Irradiation levels were recorded
 173 via SpectraWiz spectrometer software (OS v5.33, 2014, StellarNet Inc, Florida, USA). The
 174 obtained grid point values were interpolated cubically over the irradiated area to calculate the
 175 incident irradiance.

176 To start the test, a glass bead (3 mm) was placed inside each microplate well to ensure proper
177 mixing within the shaker before the wells were filled to maximum capacity with liquid (and
178 inoculum) to minimise the presence of oxygen. The microplate was carefully sealed with a
179 transparent, non-O₂ permeable, adhesive film (MicroAmp™ Optical Adhesive Film, In Vitro
180 Technologies, Australia), avoiding the formation of bubbles between the liquid and the film to
181 ensure correct optical readings. The boxes containing the microplates were placed in a
182 temperature-controlled Shaker (ThermoFisher-MAXQ4000-Incubator-110, Thermo Fisher
183 Scientific, Massachusetts, and the USA), and experiments were conducted at ~28 °C and 150
184 rpm.

185 Microplate tests were performed to acquire in-vivo UV spectra data and to extract samples for
186 carotenoid extraction followed by spectrophotometric and UPLC-UV-HRMS analyses. Five
187 microplates were inoculated with a 10 vol% of PPB inoculum, fed with Ormerod media
188 containing 500 mg COD·L⁻¹ of acetic acid. The microplates were illuminated with different IR
189 light intensities (dimable LEDs) (*i.e.*, at 1.7, 5.7, 14.2, and 33.1 W·m⁻² (later referred to as 5
190 batch tests in microplates). A non-illuminated dark control microplate was executed in
191 equivalent non-illuminated setups. Full wavelength scans (1-1000 nm) were performed every
192 5 h approximately, in a plate reader (CLARIOstar Plus, BMG Labtech) of the whole-cell (WC),
193 in-vivo and previous to any pigment extraction. To follow biomass growth, the optical density
194 at 660 nm was used as a PPB biomass proxy (OD₆₆₀) (Figure S2). Wells were sacrificially
195 sampled from random locations at t_{10} , t_{20} , t_{30} h after incubation, and at t_{final} (~55 h). The sample
196 at t_0 was taken from the bulk initial mixture. Samples were extracted from the wells with a
197 syringe with a needle, to avoid removing the film covering the microplate. Approximately 2 mL
198 of sample was immediately filtered with a 0.45 mm membrane filter (Millipore, Millex®-HP) for
199 SCOD analysis. The remaining unfiltered sample was stored at -20 °C and later used to
200 measure TCOD, TC (via spectrophotometry), and BChl a, neurosporene, and lycopene
201 contents, through UPLC-MS. TCOD and SCOD were determined by COD cell test (Merck,
202 1.14541.0001). TS/VS were determined according to

203 Standard Methods [24].

204 **2.3 Pigment analysis**

205 *2.3.1 Analytical standards preparation*

206 BChl a and lycopene were acquired from Sigma-Aldrich Pty Ltd (Castle Hill, NSW, Australia).
207 Neurosporene was purchased from Novachem (Heidelberg West, VIC, Australia). To prepare
208 stock solutions, lycopene and neurosporene analytical standards were dissolved in
209 hexane/2% CH₂Cl₂ and BChl was dissolved in methanol. To ensure preservation, 1%
210 butylated hydroxytoluene (BHT) was added to the standards, and the stock solutions were
211 flushed with argon and stored in amber vials at -20 °C. The exact concentration of each stock
212 solution was determined by UV photometry, using the absorption coefficients (mM⁻¹·cm⁻¹) 185,
213 159.4, and 54.8 for lycopene, neurosporene, and BChl a respectively, and by measuring the
214 absorbance of each compound at 470 nm, 438 nm and 771 nm using a UV-VIS
215 spectrophotometer (Cary 50 conc, Varian) [25-27].

216 *2.3.2 Pigment extraction*

217 Pigment extraction was carried out following Ruivo et al. (2012) [12], using a mixture of
218 acetone/methanol (7:2 v/v), and with the following modifications: i) the first supernatant
219 obtained by a first liquid-liquid extraction was discarded, as it resulted in no pigment recovery.
220 However, the addition of this step decreased variability between replicates in the following
221 extractions, indicating that this first extraction may serve as a wash-up step to remove other
222 polar components in the mixture that may interfere with the detection of carotenoids; (Figures
223 S1A and S1B); ii) wet biomass extract was used, as higher pigment recovery was obtained in
224 comparison to freeze-dried biomass extracts. Both wet and freeze-dried biomass samples
225 were kept at -20 °C until extraction. There was also less variability between replicates when
226 using wet biomass compared to freeze-dried biomass (data not shown); iii) samples were
227 centrifuged at a centrifugal force of 3270 x g using an Allegra X-12 centrifuge (Beckman
228 Coulter, Australia) and ultasonicated with a 10 L bath sonicator (100 W ultrasonic power,
229 FXP14, Unisonics, Australia) at a frequency of 40 kHz. Ultrasonication and centrifugation

230 times were fixed to 10 and 20 minutes, respectively, as longer times did not result in a
231 significant increase in extracted pigments (data not shown); iv) the number of full extraction
232 cycles from one sample was fixed to three, as it was found to be sufficient to recover most of
233 the contained pigments (Figure S1C).

234 2.3.3 Pigment analysis by UPLC-UV-HRMS of BChl a (BChl-Ex-UPLC) and lycopene 235 (Lyc-Ex-UPLC)

236 A UPLC-UV-HRMS method for separating, detecting and quantifying pigments was
237 developed, including BChl a of the extract by UPLC (BChl-Ex-UPLC) and lycopene of extract
238 by UPLC (Lyc-Ex-UPLC). The UPLC separation was carried out on an UltiMate 3000 Rapid
239 Separation (RS) UPLC system (Thermo Fisher Scientific, Bremen, Germany), equipped with
240 an RS pump, a temperature control column compartment, an autosampler, and a variable
241 wavelength detector. A Thermo Fisher Scientific AcclaimTM C30 (2.1 mm x 250 mm; 3.0 μ m)
242 column was used for the liquid chromatography (LC) separation. The LC parameters consisted
243 of 0.1% formic acid and 10 mmol ammonium formate (NH_4COO^-) in methanol (MeOH) as
244 mobile phase A (MP A), and 100 % methyl-tert-butyl ether (MTBE) as mobile phase B (MP B),
245 running at 0.2 mL \cdot min⁻¹, column oven temperature at 20.0 °C, and an injection volume of 15.0
246 μ L. The starting mobile phase condition was 95%:5% (MP A:MP B) at 0.0 min and hold for 2.0
247 min before gradually increase to 90%:10% (MP A:MP B) at 4.0 min, followed by 60%:40% at
248 6.0 min, 50%:50% at 13.0 min, 40%:60% at 18.0 min and eventually to 1%:99% (MP A:MP B)
249 at 22.0 min and hold for 1.0 min until 23.0 min. Then, the solvent composition was adjusted
250 back to the starting condition by increasing the MP A composition from 1% at 23.0 min to 50%
251 at 24 min and 95.0% at 26.0 min. Finally, MP A: MP B was maintained at 95%:5% for the last
252 4 min before completing the chromatography at 30.0 min. A Q-Exactive mass spectrometer
253 (Thermo Fisher Scientific, Bremen, Germany) with an Atmospheric Pressure Chemical
254 Ionization (APCI) probe. The MS data were collected in the full scan positive mode at 70,000
255 FWHM mass resolution, scanning from 150 to 2000 m/z. The automatic gain control target
256 was set at $3.0 \cdot 10^6$ and the maximum injection time at 200 ms. The source settings were as

257 follow: spray voltage at 3,500 (+), the capillary temperature at 256 °C, sheath gas at 48
258 arbitrary units (arb), auxiliary (aux) gas flow rate at 11 arb, aux gas heater temperature at 413
259 °C, S-lens radio frequency level at 50, and sweep gas flow rate at 2 arb. A 5 µg·mL⁻¹ mass
260 accuracy window was set for the mass extraction and detection setting. The UPLC-UV-HRMS
261 system was controlled by Xcalibur™ 4.1, and the MS data were processed using
262 TraceFinder™ 4.1 software. Peaks were identified by comparing the retention times, MS, and
263 UV–VIS spectral data with those of the corresponding standards. For lycopene, the 537.4455
264 m/z was used as the quantification peak and 538.4489 m/z (the ¹³C isotope peak) as the
265 confirmation peak. UV was quantified at 470 nm. The developed method was validated in
266 terms of recovery. For the validation, and to test recovery, samples of pigment-free PPB
267 biomass, which pigments had been previously extracted, were spiked with low, medium, and
268 large concentrations of a mixed solution of known concentrations of analytical standards. The
269 spiked sample with low concentration contained 0.3 µg·mL⁻¹ lycopene and 3.6 µg·mL⁻¹ BChl,
270 the medium concentrations sample had 1 µg·mL⁻¹ lycopene and 10 µg·mL⁻¹ BChl, and the
271 high concentration samples had 3 µg·mL⁻¹ lycopene and 25 µg·mL⁻¹ BChl. Lower
272 concentrations of neurosporene (1 ng·mL⁻¹, 2 ng·mL⁻¹, and 20 ng·mL⁻¹) were spiked based on
273 the amount detected in PPB samples. The spiked samples were then extracted as described
274 before. After performing UPLC-UV-HRMS analysis, the recovery of each carotenoid was
275 calculated. The UPLC-DAD analysis was carried out on an Agilent 1290 Infinity UPLC system
276 equipped with a 1290 binary pump, an auto-sampler, a column oven, and a diode array
277 detector (DAD). The chromatography conditions and column used for the UPLC-DAD analysis
278 were identical to the UPLC-UV-HRMS analysis mentioned earlier. The DAD data were
279 collected from 190-640 nm range.

280 *2.3.4 Pigment analysis by spectrophotometry of TC (TC-Ex-Abs) and BChl (BChl-Ex-* 281 *Abs)*

282 TC and BChl extracts were determined by absorbance (TC-Ex-Abs and BChl-Ex-Abs) using
283 previously published methods [28] and a Quartz cuvette for measurements. The TC content

284 was calculated using the absorbance of the extracted pigments at 475 nm and using the
285 spirilloxanthin extinction coefficient ($94 \text{ mM}^{-1}\cdot\text{cm}^{-1}$). The molecular weight of spirilloxanthin
286 ($596.94 \text{ g}\cdot\text{mol}^{-1}$) was used to obtain the concentration of TC in $\text{mg}\cdot\text{g}^{-1}$. BChl content was
287 calculated by measuring absorbance at 771 nm, assuming a molar extinction coefficient of
288 $65.3 \text{ mM}^{-1}\cdot\text{cm}^{-1}$ [29]. The cuvette path length of 1 cm was used for all calculations.

289 **2.4 Microbial analysis**

290 The microbial composition of samples collected at the end of each batch test was analysed
291 via genomic sequencing by the Australian Centre for Ecogenomics (ACE). DNA extraction as
292 per Qiagen DNeasy Powersoil Kit and amplification were conducted by ACE. The universal
293 primer pair Univ_ SSU_ 926F-1392wR was used, targeting regions of the 16S and 18S rRNA
294 genes [30]. Sequencing was conducted using the Illumina® platform. Reads identified as a
295 single read, with a relative abundance of less than 0.05% or sequence identity less than 60%
296 were discarded. Raw Illumina amplicon sequencing reads across samples were processed
297 using the DADA2 package (version 1.16) in R (version 4.0.2) to infer amplicon sequencing
298 variants (ASV) and their relative abundance. The taxonomic affiliation of the ASVs was
299 assigned in DADA2 with the SILVA rRNA gene database (version 138).

300 **2.5 Data processing and statistical analysis**

301 The measured results are presented as averages, and their variability is expressed as
302 standard deviation, given as $\bar{X}(S_{X_i})$ where \bar{X} , is the average value for the data X_i , and S_{X_i} is
303 the corresponding standard deviation. The calculated parameters are presented as average
304 values, with uncertainty expressed as uncertainty in the mean value based on a two-tailed t-
305 test at the 95% confidence level and with an appropriate number of degrees of freedom. Thus,
306 values are given below as $\bar{X} \pm E_{\bar{X}}$, where $E_{\bar{X}}$ is the estimated error at a 95% confidence level.

307 *2.5.1 Analysis of whole-cell spectra (Lyc-WC-PCA, BChl-WC-PCA)*

308 The spectrum ranges of 450-550 nm (1 nm spacing), obtained across the 25 observations,
309 corresponding to the 5 light conditions (0, 1.7, 5.7, 14.2, and $33.1 \text{ W}\cdot\text{m}^{-2}$) at 5 time-points
310 each, were decomposed across the 25 observations by PCA on the 100 evenly spaced

311 spectral amplitudes. The top 20 principal components (of 100) were regressed (see below).
312 Both the whole-cell and extract spectra were analysed, but only the whole-cell results are
313 presented here. Spectrum PCs were assessed for their ability to predict UPLC results on all
314 samples analysed for extracted BChl (BChl-Ex-UPLC) and extracted lycopene (Lyc-Ex-
315 UPLC). Similarly, the capability of spectrophotometric-absorbance measures of extracted TC
316 (TC-Ex-Abs) and BChl (BChl-Ex-Abs) to predict UPLC-UV-HRMS results was assessed. TC-
317 Ex-Abs and BChl-Ex-Abs were centred on the lycopene and BChl means (*i.e.*, TC and BChl
318 means and slopes were normalised) to best estimate their ability to predict BChl and Lyc
319 contents, and allow a consistent comparison to PCA based predictions (see below). This was
320 done on all 25 whole-cell samples, and on the 20 extracted samples.

321 PCAs (with centred covariance) were performed using Matlab 2020b (function `pca()`).
322 Correlation analysis (function `Correl()`) in Excel 16 was used to determine which combination
323 of PCs could be used as a predictor for measured values, and the general linear model in
324 Excel 16 (function `list()`) was used to build models for UPLC (BChl-Ex-UPLC) and Lycopene
325 (Lyc-Ex-UPLC) concentrations from PCs without considering interaction or parabolic effects.

326 **3 Results and discussion**

327 **3.1 Neurosporene, lycopene and BChl detection and quantification through UPLC- 328 UV-HRMS: method development and recovery efficiency**

329 The mean lycopene recovery from 6 spiked samples at the three different spike levels (0.30,
330 1.02, and 3.00 $\mu\text{g}\cdot\text{g}^{-1}$) were 97.5%, 85.0%, and 83.8% analysed under full scan HRMS and
331 98.7%, 82.2 %, and 87.0% at UV 470 nm (Table 1). Both HRMS and UV detection gave very
332 similar average recoveries across the three different spiked levels at 88.8% and 89.3%. The
333 average relative standard deviations (RSD) calculated from the mean recoveries for the
334 HRMS, and UV detections were 8.6% and 9.6%, suggesting that both methods have good
335 precision and reproducibility (average RSDs <10%). The mean neurosporene recoveries were
336 88.5%, 96.3%, and 113.7% at the three different spiked levels (0.002, 0.005, and 0.020 $\mu\text{g}\cdot\text{g}^{-1}$)
337 ¹), respectively for HRMS detection (UV detection was not sensitive enough at the spiked

338 levels). BChl showed a lower mean recovery (73.6% and 82.1% for HRMS and UV,
339 respectively), which may be linked to its rapid degradation or an insufficient extraction.

340

341 **Table 1.** Recovery of neurosporene, lycopene, and BChl as measured by UPLC-UV_HRMS
342 (n = 6 at each spiked level).

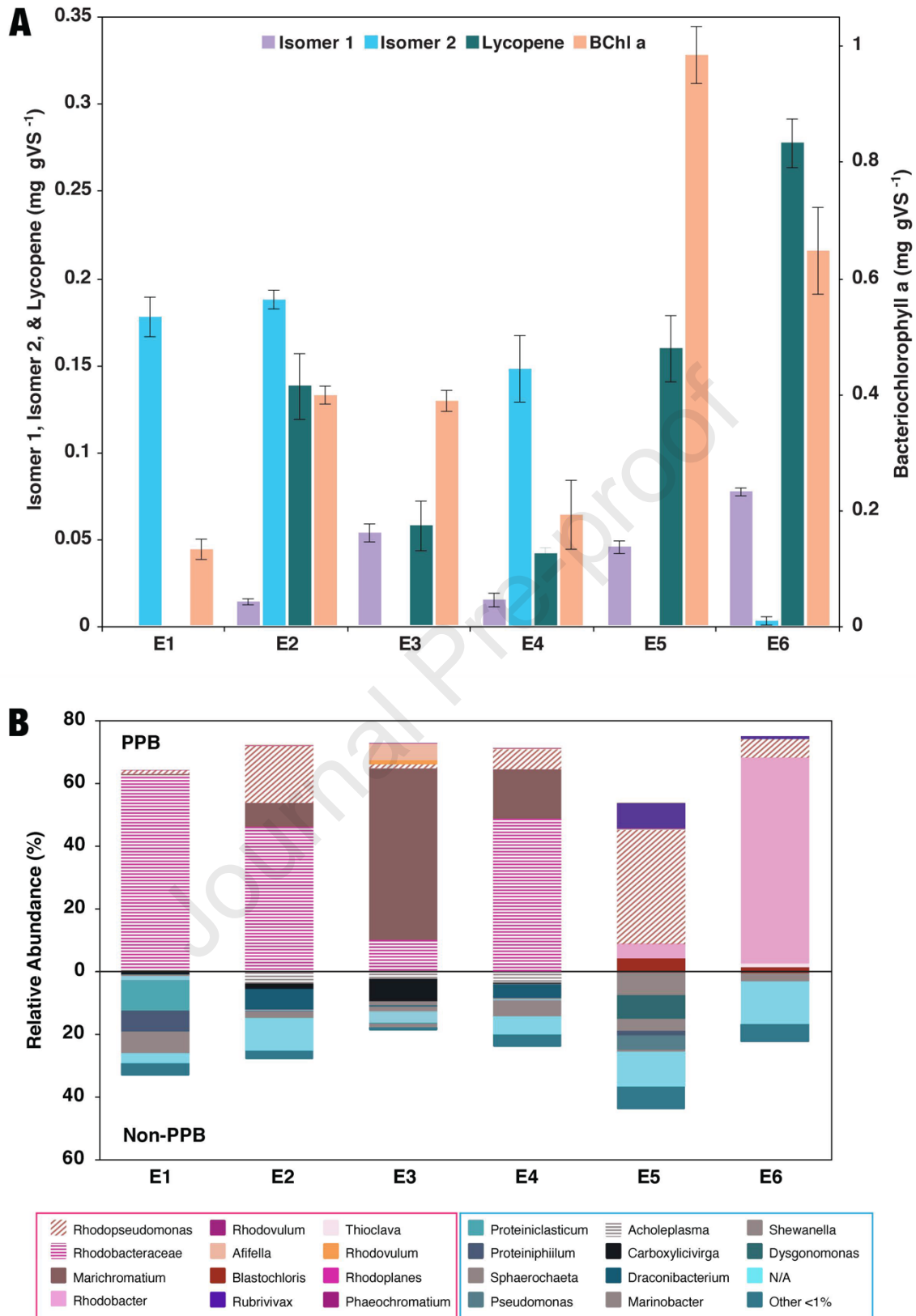
Analyte	Spiking Level, $\mu\text{g}\cdot\text{g}^{-1}$	Detected $(\bar{X}(S_{Xi})), \mu\text{g}\cdot\text{g}^{-1}$	Recovery $(\bar{X}(S_{Xi})), \%$	Avg Recovery $(\bar{X}(S_{Xi})), \%$	RSD, %
Lycopene					
HRMS	0.30	0.29 (0.04)	97.5 (13.3)	88.8 (7.6)	8.6
	1.02	0.87 (0.12)	85.0 (11.6)		
	3.00	2.52 (0.49)	83.8 (16.3)		
UV	0.30	0.30 (0.04)	98.7 (12.8)	89.3 (8.5)	9.6
	1.02	0.84 (0.13)	82.2 (12.3)		
	3.00	2.61 (0.48)	87.0 (16.0)		
Neurosporene					
HRMS	0.002	1.77 (0.24)	88.5 (11.8)	99.5 (12.5)	12.6
	0.005	4.82 (0.23)	96.3 (4.5)		
	0.020	22.7 (0.32)	113.7 (1.6)		
BChl a					
HRMS	5.15	4.52 (0.55)	87.7 (10.6)	73.6 (12.6)	17.1
	20.13	14.03 (2.21)	69.7 (11)		
	50.14	31.78 (3.83)	63.4 (7.6)		
UV	5.15	5.52 (1.66)	107 (32.2)	82.1 (21.7)	26.4
	20.13	14.52 (2.95)	72.1 (14.7)		
	50.14	33.69 (4.48)	67.2 (8.9)		

343

344 3.2 UPLC-UV-HRMS detection and quantification of pigments in PPB enrichments

345 Several PPB cultures enriched from domestic wastewater, poultry processing wastewater,
346 Brisbane River, and sediments (E1-E6; described in 2.1) were analysed for their pigment
347 contents. Representative isotropic profiles of lycopene (M+H) ($\text{C}_{40}\text{H}_{56}$), and a comparison of
348 the chromatograms from the lycopene standard (retention time of 20.7 min), from the lycopene
349 present in a PPB sample monitoring the lycopene molecular ion (537.4455 m/z, black peak),
350 and the isotope ion (538.4489 m/z, red peak), are presented in Figure S3. All the enrichments
351 except for E1 contained lycopene, eluting at 20.8 min as in the analytical standard (all-
352 trans lycopene). However, the method also enabled the detection of two other lycopene-like
353 compounds, eluting at 16.38 and 17.6 min and designated as isomer 1 and isomer 2 (Figure

354 2A). Although different lycopene isomers have been widely studied in dietary sources such as
355 tomato, and human serum and tissues, this is the first time that the detection and quantification
356 of different lycopene isomers in PPB are described in the literature. The isomers content varied
357 between samples, most likely because of the different PPB communities resulting from the
358 different inoculum sources and growth conditions (Figure 2B). While *Rhodopseudomonas sp.*
359 and *Rhodobacter sp.* (dominant in piggery wastewater (E5) and domestic wastewater (E6))
360 showed a similar isomer distribution (mainly the all-trans lycopene), samples with dominant
361 *Rhodobacteraceae* also showed the presence of an isomer 2 peak, in higher concentrations
362 than all-trans lycopene. Although neurosporene was detected in negligible amounts in PPB
363 enrichments, the method may be relevant in the future to enable the analysis of this compound
364 under different growth conditions. While other illumination sources including UV-VIS might
365 impact individual carotenoids, NIR generally produces both, BChl and carotenoids as relevant
366 genes for their synthesis are grouped in photosynthetic gene cluster (PGC) [31-34]. In fact,
367 carotenoids are essential for the formation of the light harvesting complexes (LHC) [11]



368

369 **Figure 2.** (A) Distribution of the three major lycopene isomers detected at RT: 16.38 (isomer

370 1), 17.6 (isomer 2), and 20.8 min (lycopene) among 6 PPB mixed cultures enriched from

371 sediments from Tuckean Broadwater and sea salt addition of 30 mS (E1), Ballina Mangrove
 372 Habitat and salt addition of 30 mS (E2) and 70 mS (E3), Brisbane River (E4), poultry
 373 processing wastewater (E5) and domestic wastewater (E6). (B) Relative abundance of
 374 different microbial communities corresponding to each of the enriched PPB cultures.

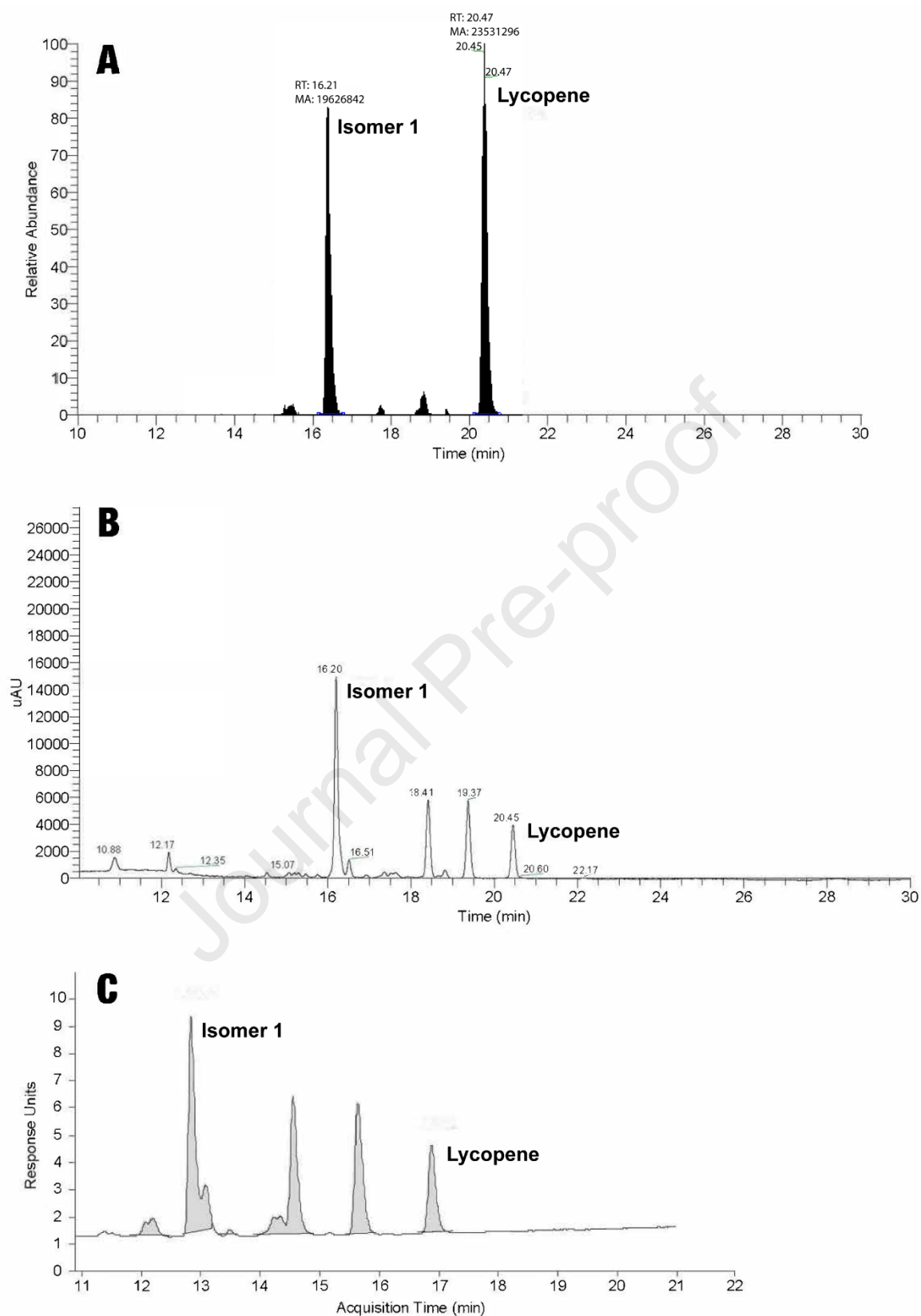
375 The UV spectra for lycopene, isomer 1, and isomer 2 were obtained by running the samples
 376 (E1-E6) through UPLC coupled with a DAD detector. The UPLC-DAD chromatogram at 470
 377 nm, the UPLC-UV chromatogram, and the UPLC-HRMS chromatogram of each PPB
 378 enrichment sample were compared to identify the peaks with m/z corresponding to lycopene
 379 and thus be able to access the individual UV spectra, as shown in Figure 3 for sample E3.
 380 Three different UV spectra profiles were observed for each compound (lycopene, isomer 1,
 381 and isomer 2) when matching the UV chromatogram from the two different instruments (MS
 382 and DAD) in all the PPB enrichment samples (see Table 2 and Figure S4). Isomer 2 and
 383 lycopene showed a very similar UV spectrum; however, their distinct elution times (16.3 and
 384 20.8 min) make isomer 2 a lycopene isomer candidate (see Figure S5 for an example with
 385 isomer 2). Isomer 1 had a more distinct UV spectrum, with maximum absorbance peaks
 386 shifted to shorter wavelengths when compared to isomer 2 and lycopene. Although this
 387 method enabled the detection of different lycopene isomers, there are no available analytical
 388 standards for accurate identification of the isomers and further isolation and structural
 389 elucidation (e.g. by using NMR) should be performed to fully elucidate these compounds.

390

391 **Table 2.** Identification data for lycopene isomers.

Lycopene Isomer	RT (min)	λ max (nm)			
Isomer 1	16.3	280	430	454	487
Isomer 2	17.6	294	446	472	504
Lycopene	20.8	294	446	470	502

392



393

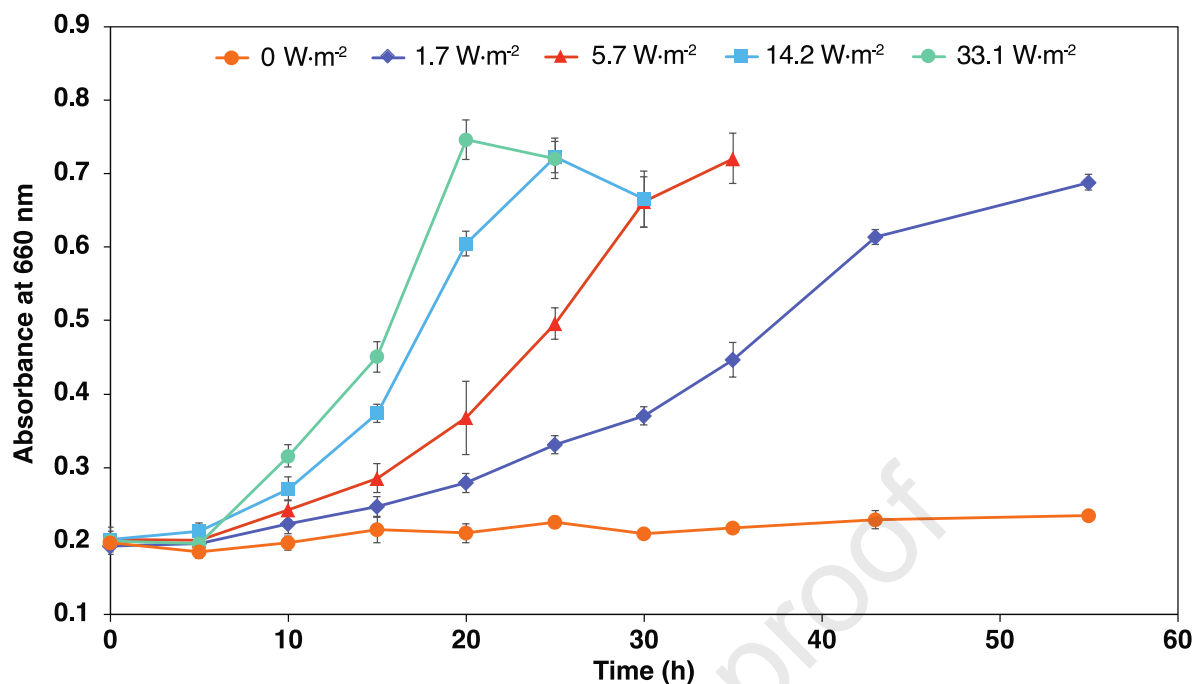
394 **Figure 3.** Composition analyses of lycopene in E3. (A) UPLC-MS chromatogram at 537 m/z,

395 (B) UPLC-UV chromatogram at 470 nm, and (C) UPLC-DAD chromatogram at 470 nm.

396 The combined lycopene contents did not exceed 0.3 mg lycopene·g VS⁻¹ (combined isomers),
397 which is on the lower end of literature values where up to 2 mg g⁻¹ (dry weight) was reported
398 for the purple phototrophic bacterium *Rhodospirillum rubrum* after genetic manipulation [35],
399 and up to 18 mg g⁻¹ (dry weight) were reported in other genetically engineered microorganisms
400 [36]. At this stage, we cannot state standard lycopene contents of mixed PPB cultures under
401 non-engineered conditions. The data show that the UPLC-UV-HRMS method can be used to
402 analyse the lycopene content in environmental samples, with greater accuracy compared with
403 spectrophotometric methods. Due to the use of a polymeric C₃₀ column, the developed method
404 also enables lycopene isomers separation, which cannot be resolved by the commonly used
405 C₁₈ columns [37]. Different isomers have varying functions and potencies [38, 39], which
406 makes the isomer identification relevant to assess the potential absorption and health benefits
407 of the lycopene produced in PPB cultures, e.g. when used as SCP in feed. For example, the
408 antioxidative properties of cis-lycopene have been reported inferior to all-trans-lycopene [38].
409 On the other side, cis-isomers have repeatedly been shown to be substantially more
410 bioavailable than all-trans lycopene [16].

411 3.3 Plate reader tests and spectral decomposition-based analysis

412 The microplate set-up enabled the recording of PPB photoheterotrophic growth in 12 well
413 microplates. Growth curves were recorded by measuring OD₆₆₀ in a plate reader (with an
414 acceptable CI95%). OD₆₆₀ measurements for the four light intensities over time are shown in
415 Figure 4. This is an effective predictor for particulate COD (R² = 0.9908), shown in Figure S2,
416 which can be used as biomass proxy, especially in clean substrate tests (without native
417 particulate COD due to serial dilutions). Additionally, each well's absorbance spectrum was
418 scanned to monitor characteristic peaks of carotenoids (400-500 nm) and BChl a (800-900
419 nm).



420

421 **Figure 4.** PPB growth curves measured as OD₆₆₀ in microplates using different light intensities
 422 (0, 1.7, 5.7, 14.2, and 33.1 W·m⁻²).

423 Time series whole-cell spectra collected during experiments in the microplates were
 424 decomposed via covariance PCA as noted in the methods (2.5.1). The vast majority of
 425 covariance was held in PC1 (99.97%), which was related to change in overall spectrum
 426 amplitude. This effectively removes the background of general cellular material. Of the
 427 remaining covariance, 99.999% was contained in PCs 2-10.

428 A full correlation table of Lycopene and BChl via UPLC-UV-HRMS (Lyc-Ex-UPLC and BChl-
 429 Ex-UPLC), to the individual spectral PCs for whole-cell and extract is given in Table S1. Lyc-
 430 Ex-UPLC was correlated with PC2, PC3, and PC12, while BChl-Ex-UPLC was correlated with
 431 PC2, PC8, and PC13 (and to a lesser extent, PC1 and PC10). PC2 therefore likely contains
 432 common features to both BChl and Lyc, but it is important to note that the other PCs are
 433 different, and BChl and Lyc can be fitted separately using different features. To develop a
 434 predictive model for Lyc-Ex-UPLC and BChl-Ex-UPLC from the spectral PCs, data were
 435 randomly split into fitting (20 points) and validation (5 points). Increasing the number of
 436 predictors (PCs) as inputs to the model improved the R² to the fit points (up to 0.99) but caused

437 validation to become excessively poor, likely because PCs were used to improve fits on
 438 individual points with excessive empirical inputs. To address this, the number of predictors
 439 was limited to achieve similar R^2 values between fitting and validation data sets, and in each
 440 case, this resulted in 3 predictors. The optimised models and individual parameter p-values
 441 are shown in Table 3. The low p-value for PC8 indicates it could be eliminated in the model
 442 for BChl-Ex-UPLC, but this resulted in the fit R^2 value dropping to 0.73 (from 0.77) without an
 443 improvement in validation R^2 . Analysis of the extract PC spectroscopy resulted in similar model
 444 qualities (with an increased contribution from PC1 and decreased variance in PC1). Because
 445 it was not superior to the whole-cell PCA and is considerably more effort (requiring solvent
 446 extraction), it is not presented here (but included as Table S1).

447 **Table 3.** Whole-cell PCA models for Lycopene and BChl by UPLC (Lyc-Ex-UPLC and BChl-
 448 Ex-UPLC).

PCA-Lycopene Model				
Predictor	PC2	PC3	PC12	Intercept
Parameter	-6.06±0.67	-15.20±4.9	199±137	0.70
p-value	1x10 ⁻¹⁴	3x10 ⁻⁶	8x10 ⁻³	
PCA-BChl Model				
Predictor	PC2	PC8	PC13	Intercept
Parameter	-25.2±5.0	-520.9±419	-1627.2±690	6.87
p-value	8x10 ⁻¹⁰	2x10 ⁻²	1x10 ⁻⁴	

449 Uncertainty in parameters (\pm) are 95% confidence intervals

450 The correlation table for the three methods (Ex-UPLC, Ex-Abs, WC-PCA) and two target
 451 compounds are shown in Table 4. The Ex-Abs values required significant correction by
 452 regression to be effective predictors for the Ex-UPLC measures (particularly TC to Lyc) and
 453 even then, had significant issues. Correlation between extractive absorption (TC-Ex-Abs,
 454 BChl-Ex-Abs) and the UPLC methods are reasonable at $r=0.84$ and $r=0.85$ for target
 455 compounds. However, TC-Ex-Abs is also a good predictor for BChl-UPLC (*i.e.*, non-specific),
 456 which means that BChl is potentially a strong interference for the TCA method. In addition, the
 457 correlation between the two extraction-absorption (TC-Ex-Abs, BChl-Ex-Abs) was 0.91, which
 458 means that these methods interact strongly. That is, both are largely measuring the same

459 compound (total pigments) rather than separate pigments. In contrast, the correlation
 460 coefficient for WC-PCA methods was higher than for the Ex-Abs methods in both cases (to
 461 UPLC), and PCA was more specific to the target compound. UPLC (Ex-UPLC) results vs
 462 predictions from the whole-cell spectral PCA (WC-PCA) are shown in Figure S6A for TC, and
 463 S5B for BChl.

464 As noted in the methods, due to loss of some extracted individual replicates (due to limited
 465 sample volumes), averages of technical triplicates for spectra, UPLC measurements, etc.
 466 were used. To validate this for individual samples, the same procedure was also done on
 467 individual replicates excluding zero lycopene reads (total n=63). The results were consistent,
 468 with PC2 and PC3 dominating correlation, and with an overall R^2 of 0.79. As seen in
 469 supplementary Figure S7 ($r=0.89$), most of the errors are at very low lycopene levels (where
 470 the relative uncertainty in replicate analysis was highest). Due to the increased observations,
 471 p-values were far lower ($\times 10^{-3}$) than shown in Table 3.

472

473 **Table 4.** Comparison of different methods to assess Lycopene and BChl (Pearson correlation
 474 coefficient of parity model).

	Lyc-Ex-UPLC	BChl-Ex-UPLC
Lyc-Ex-UPLC	<u>1.00</u>*	0.66
BChl-Ex-UPLC	0.66	<u>1.00</u>
TC-Ex-Abs	<u>0.84</u>	0.87
BChl-Ex-Abs	0.69	<u>0.82</u>
Lyc-WC-PCA	<u>0.88</u>	0.60
BChl-WC-PCA	0.68	<u>0.86</u>

475 *Target of analytical method is underlined and bold. Correlation between TC-Ex-Abs and BChl-Ex-Abs
 476 is 0.92. Colours indicate correlation.

477 The absorbance of extract, while effective for plant samples, where the carotenoid profile is
 478 known, is non-selective in microbial cultures. Limited improvement in the method is unlikely,
 479 while whole-cell PCA has been analysed with only 25 (averaged triplicate) samples from 5
 480 microplates batch tests (described in section 2.2 at different wavelengths) and will improve

481 substantially as more samples can be analysed. Both are subject to matrix issues, which may
482 include the flanking community, background coloured compounds (e.g., humics, cellular
483 polymers, etc), but this can be corrected in PCA. PCA on whole-cell spectrum can be done on
484 live cells, during the experiment, or for a pigment production platform, at an industrial scale,
485 and does not require pigment extraction. When the matrix changes, a large number of whole-
486 cell spectra can be fit using a relatively small number of UPLC measurements, and this can
487 be continuously updated, with error analysis continuously applied. As far as we are aware,
488 this is the first instance of full spectra decomposition by PCA and comparison against chemical
489 analysis. Other methods, such as the Gauss-peak spectra method, have been applied to
490 qualify and quantify individual pigments from total absorbance spectra from higher plants,
491 brown algae, *Euglena*, *Trichodesmium*, and *Anabaena*. However, standards are necessary to
492 calibrate the methods (a spectrum fitting library is available) [40], which limits the application
493 for specific PPB pigments.

494 While UPLC remains the “best” technique, it is limited in terms of analytes. This is because
495 other carotenoids produced by PPB such as spirilloxanthin or okenone do not have readily
496 available commercial standards, which is a prerequisite for their reliable detection and
497 quantification e.g. with UV-HRMS detectors [21]. Increased interest in the PPB platform will
498 likely drive the availability of standards that can be used to calibrate the PCA method for
499 various individual carotenoids. This would enable high throughput methods e.g. to screen the
500 best conditions to accumulate specific carotenoids or control industrial production in mixed or
501 pure cultures. We note the PCA calibration will be required to include matrix effects of different
502 wastewaters and different communities and variability need to be further assessed.

503 **4 Conclusions**

504 Studies to optimise the biosynthesis of carotenoids in purple phototrophic bacteria require a
505 reliable analytical method that enables the detection and quantification of individual
506 carotenoids and their isomers. The UPLC-UV-HRMS method presented here was reliable for
507 the quantitative determination of neurosporene, lycopene, and BChl a. These compounds

508 were separated on a reverse-phase C₃₀ carotenoid column, enabling the detection of three
509 different lycopene isomers. Compared to traditional spectrophotometric methods, this method
510 has the advantages of detecting individual carotenoids and of providing accurate identification
511 due to the use of analytical standards. Full identification of other carotenoids present in the
512 sample requires suitable standards, but the m/z and UV Spectra data could be used for
513 tentative identification of the other carotenoids. The classic extraction-absorption method was
514 not particularly effective in separating different pigments and had matrix effects. However,
515 analysing whole-cell spectra via PCA allowed more accurate prediction of individual pigments,
516 and can be done non-destructively, during live-cell growth. It does require calibration for media
517 and microbial matrices, but once calibrated, is a rapid, and relatively low effort method.

518

519 **Acknowledgements**

520 This project is supported by Meat and Livestock Australia through funding from the Australian
521 Government Department of Agriculture, Water and the Environment (RnD4Profit-16-03-002)
522 as part of its Rural R&D for Profit program and the partners. Gabriel Capson-Tojo
523 acknowledges the Xunta de Galicia for his postdoctoral fellowship (ED481B-2018/017). We
524 would like to recognise the work of Sam Grieve and UQ Innovate team who collaborated on
525 the design of the microplate set-up, and Tom Mason who helped with the LED lighting system.

526

527 **References**

- 528 [1] J. Yabuzaki, Carotenoids Database: structures, chemical fingerprints and distribution among
529 organisms, Database 2017 (2017)
- 530 [2] J. Nagarajan, R.N. Ramanan, M.E. Raghunandan, C.M. Galanakis, N.P. Krishnamurthy, Carotenoids,
531 Nutraceutical and Functional Food Components: Effects of Innovative Processing Techniques (2017)
532 259-296. <https://doi.org/10.1016/B978-0-12-805257-0.00008-9>
- 533 [3] B. Capelli, D. Bagchi, G.R. Cysewski, Synthetic astaxanthin is significantly inferior to algal-based
534 astaxanthin as an antioxidant and may not be suitable as a human nutraceutical supplement,
535 Nutrafoods 12(4) (2013) 145-152. <https://doi.org/10.1007/s13749-013-0051-5>
- 536 [4] C.K. Venil, Z.A. Zakaria, W.A. Ahmad, Bacterial pigments and their applications, Process Biochem
537 48(7) (2013) 1065-1079. <https://doi.org/10.1016/j.procbio.2013.06.006>

- 538 [5] M.Y. Gong, A. Bassi, Carotenoids from microalgae: A review of recent developments, *Biotechnol*
539 *Adv* 34(8) (2016) 1396-1412. <https://doi.org/10.1016/j.biotechadv.2016.10.005>
- 540 [6] K. Ludwig, L. Rihko-Struckmann, G. Brinitzer, G. Unkelbach, K. Sundmacher, β -Carotene extraction
541 from *Dunaliella salina* by supercritical CO₂, *Journal of Applied Phycology* 33(3) (2021) 1435-
542 1445. <https://doi.org/10.1007/s10811-021-02399-y>
- 543 [7] L. Novoveská, M.E. Ross, M.S. Stanley, R. Pradelles, V. Wasiolek, J.-F. Sassi, Microalgal Carotenoids:
544 A Review of Production, Current Markets, Regulations, and Future Direction, *Marine Drugs* 17(11)
545 (2019)
- 546 [8] G. Capson-Tojo, D.J. Batstone, M. Grassino, S.E. Vlaeminck, D. Puyol, W. Verstraete, R.
547 Kleerebezem, A. Oehmen, A. Ghimire, I. Pikaar, J.M. Lema, T. Hulsen, Purple phototrophic bacteria for
548 resource recovery: Challenges and opportunities, *Biotechnol Adv* 43
549 (2020). <https://doi.org/10.1016/j.biotechadv.2020.107567>
- 550 [9] T. Hülsen, E.M. Sander, P.D. Jensen, D.J. Batstone, Application of purple phototrophic bacteria in a
551 biofilm photobioreactor for single cell protein production: Biofilm vs suspended growth, *Water*
552 *Research* 181 (2020) 115909. <https://doi.org/10.1016/j.watres.2020.115909>
- 553 [10] M.T. Madigan, D.O. Jung, An Overview of Purple Bacteria: Systematics, Physiology, and Habitats,
554 in: C.N. Hunter, F. Daldal, M.C. Thurnauer, J.T. Beatty (Eds.), *The Purple Phototrophic Bacteria*,
555 Springer Netherlands, Dordrecht, 2009, pp. 1-15. [10.1007/978-1-4020-8815-5_1](https://doi.org/10.1007/978-1-4020-8815-5_1)
- 556 [11] A.A. Moskalenko, Z.K. Makhneva, Light-harvesting complexes from purple sulfur bacteria
557 *Allochrochromatium minutissimum* assembled without carotenoids, *J Photochem Photobiol B* 108 (2012)
558 1-7. <https://doi.org/10.1016/j.jphotobiol.2011.11.006>
- 559 [12] M. Ruivo, P. Cartaxana, M.I. Cardoso, A. Tenreiro, R. Tenreiro, B. Jesus, Extraction and
560 quantification of pigments in aerobic anoxygenic phototrophic bacteria, *Limnol Oceanogr-Meth* 12
561 (2014) 338-350. <https://doi.org/10.4319/lom.2014.12.338>
- 562 [13] S. Takaichi, Characterization of carotenes in a combination of a C18HPLC column with isocratic
563 elution and absorption spectra with a photodiode-array detector, *Photosynth Res* 65(1) (2000) 93-
564 99. <https://doi.org/10.1023/A:1006445503030>
- 565 [14] J.G. Provesi, C.O. Dias, E.R. Amante, Changes in carotenoids during processing and storage of
566 pumpkin puree, *Food Chem* 128(1) (2011) 195-202. <https://doi.org/10.1016/j.foodchem.2011.03.027>
- 567 [15] K.T. Amorim-Carrilho, A. Cepeda, C. Fente, P. Regal, Review of methods for analysis of
568 carotenoids, *Trac-Trend Anal Chem* 56 (2014) 49-73. <https://doi.org/10.1016/j.trac.2013.12.011>
- 569 [16] T.W. Boileau, A.C. Boileau, J.W. Erdman, Jr., Bioavailability of all-trans and cis-isomers of lycopene,
570 *Exp Biol Med (Maywood)* 227(10) (2002) 914-9. <https://doi.org/10.1177/153537020222701012>
- 571 [17] A. During, M.M. Hussain, D.W. Morel, E.H. Harrison, Carotenoid uptake and secretion by CaCo-2
572 cells: beta-carotene isomer selectivity and carotenoid interactions, *J Lipid Res* 43(7) (2002) 1086-
573 95. <https://doi.org/10.1194/jlr.m200068-jlr200>
- 574 [18] L.C. Sander, C.A. Rimmer, W.B. Wilson, Characterization of triacontyl (C-30) liquid
575 chromatographic columns, *J Chromatogr A* 1614 (2020)
576 460732. <https://doi.org/10.1016/j.chroma.2019.460732>
- 577 [19] K.E. Sharpless, J.B. Thomas, L.C. Sander, S.A. Wise, Liquid chromatographic determination of
578 carotenoids in human serum using an engineered C30 and a C18 stationary phase, *J Chromatogr B*
579 *Biomed Appl* 678(2) (1996) 187-95. [https://doi.org/10.1016/0378-4347\(95\)00494-7](https://doi.org/10.1016/0378-4347(95)00494-7)
- 580 [20] R.E. Kopec, J.L. Cooperstone, M.J. Cichon, S.J. Schwartz, Analysis Methods of Carotenoids, *Analysis*
581 *of Antioxidant-Rich Phytochemicals* 2012, pp. 105-148. <https://doi.org/10.1002/9781118229378.ch4>
- 582 [21] D.B. Rodriguez-Amaya, M. Kimura, I.F.P.R. Institute, C.I.d.A. Tropical, HarvestPlus Handbook for
583 Carotenoid Analysis, International Food Policy Research Institute (IFPRI)2004.
- 584 [22] T. Hulsen, K. Hsieh, D.J. Batstone, Saline wastewater treatment with purple phototrophic bacteria,
585 *Water Res* 160 (2019) 259-267. <https://doi.org/10.1016/j.watres.2019.05.060>
- 586 [23] J.G. Ormerod, H. Gest, K.S. Ormerod, Light-dependent utilization of organic compounds and
587 photoproduction of molecular hydrogen by photosynthetic bacteria - Relationships with nitrogen

- 588 metabolism, Arch Biochem Biophys 94(3) (1961) 449-&.https://doi.org/10.1016/0003-
589 9861(61)90073-X
- 590 [24] A.W.W.A.W.E.F. American Public Health Association, Standard methods for the examination of
591 water and wastewater, APHA-AWWA-WEF, Washington, D.C., 1998.
- 592 [25] K.J. Scott, Detection and Measurement of Carotenoids by UV/VIS Spectrophotometry, Current
593 Protocols in Food Analytical Chemistry 00(1) (2001) F2.2.1-
594 F2.2.10.https://doi.org/10.1002/0471142913.faf0202s00
- 595 [26] Z.B. Namsaraev, Application of extinction coefficients for quantification of chlorophylls and
596 bacteriochlorophylls, Microbiology+ 78(6) (2009) 794-
597 797.https://doi.org/10.1134/S0026261709060174
- 598 [27] S.C. Chi, D.J. Mothersole, P. Dilbeck, D.M. Niedzwiedzki, H. Zhang, P. Qian, C. Vasilev, K.J. Grayson,
599 P.J. Jackson, E.C. Martin, Y. Li, D. Holten, C.N. Hunter, Assembly of functional photosystem complexes
600 in Rhodobacter sphaeroides incorporating carotenoids from the spirilloxanthin pathway, Bba-
601 Bioenergetics 1847(2) (2015) 189-201.https://doi.org/10.1016/j.bbabi.2014.10.004
- 602 [28] H.K. Lichtenthaler, Chlorophylls and Carotenoids - Pigments of Photosynthetic Biomembranes,
603 Method Enzymol 148 (1987) 350-382
- 604 [29] M. van der Rest, G. Gingras, The Pigment Complement of the Photosynthetic Reaction Center
605 Isolated from Rhodospirillum rubrum, Journal of Biological Chemistry 249(20) (1974) 6446-
606 6453.https://doi.org/10.1016/S0021-9258(19)42177-7
- 607 [30] A. Engelbrektson, V. Kunin, K.C. Wrighton, N. Zvenigorodsky, F. Chen, H. Ochman, P. Hugenholtz,
608 Experimental factors affecting PCR-based estimates of microbial species richness and evenness, Isme
609 J 4(5) (2010) 642-647.https://doi.org/10.1038/ismej.2009.153
- 610 [31] U. Ermler, G. Fritzsche, S.K. Buchanan, H. Michel, Structure of the Photosynthetic Reaction-Center
611 from Rhodobacter-Sphaeroides at 2.65-Angstrom Resolution - Cofactors and Protein-Cofactor
612 Interactions, Structure 2(10) (1994) 925-936.https://doi.org/10.1016/S0969-2126(94)00094-8
- 613 [32] X.C. Hu, T. Ritz, A. Damjanovic, F. Autenrieth, K. Schulten, Photosynthetic apparatus of purple
614 bacteria, Q Rev Biophys 35(1) (2002) 1-62.https://doi.org/10.1017/S0033583501003754
- 615 [33] N. Igarashi, J. Harada, S. Nagashima, K. Matsuura, K. Shimada, K.V.P. Nagashima, Horizontal
616 transfer of the photosynthesis gene cluster and operon rearrangement in purple bacteria, J Mol Evol
617 52(4) (2001) 333-341.https://doi.org/10.1007/s002390010163
- 618 [34] Q. Zheng, R. Zhang, M. Koblizek, E.N. Boldareva, V. Yurkov, S. Yan, N.A.Z. Jiao, Diverse
619 Arrangement of Photosynthetic Gene Clusters in Aerobic Anoxygenic Phototrophic Bacteria, Plos One
620 6(9) (2011).https://doi.org/10.1371/journal.pone.0025050
- 621 [35] G.S. Wang, H. Grammel, K. Abou-Aisha, R. Sagesser, R. Ghosh, High-level production of the
622 industrial product lycopene by the photosynthetic bacterium Rhodospirillum rubrum, Appl Environ
623 Microbiol 78(20) (2012) 7205-15.https://doi.org/10.1128/AEM.00545-12
- 624 [36] H. Alper, K. Miyaoku, G. Stephanopoulos, Construction of lycopene-overproducing E. coli strains
625 by combining systematic and combinatorial gene knockout targets, Nat Biotechnol 23(5) (2005) 612-
626 6.https://doi.org/10.1038/nbt1083
- 627 [37] B.S. Inbaraj, J.T. Chien, B.H. Chen, Improved high performance liquid chromatographic method
628 for determination of carotenoids in the microalga Chlorella pyrenoidosa, J Chromatogr A 1102(1-2)
629 (2006) 193-199.https://doi.org/10.1016/j.chroma.2005.10.055
- 630 [38] D.E. Holloway, M. Yang, G. Paganga, C.A. Rice-Evans, P.M. Bramley, Isomerization of dietary
631 lycopene during assimilation and transport in plasma, Free Radical Res 32(1) (2000) 93-
632 102.https://doi.org/10.1080/10715760000300101
- 633 [39] M.T. Lee, B.H. Chen, Separation of lycopene and its cis isomers by liquid chromatography,
634 Chromatographia 54(9-10) (2001) 613-617.https://doi.org/10.1007/Bf02492187
- 635 [40] H. Kupper, S. Seibert, A. Parameswaran, Fast, sensitive, and inexpensive alternative to analytical
636 pigment HPLC: Quantification of chlorophylls and carotenoids in crude extracts by fitting with gauss
637 peak spectra, Anal Chem 79(20) (2007) 7611-7627.https://doi.org/10.1021/ac070236m

Highlights

- A UPLC-UV-HRMS method to detect and quantify PPB pigments was developed
- A C₃₀ column enabled detection and quantification of two lycopene isomers
- A microplate method for photoheterotrophic PPB cultivation was developed
- Pigment contents can be determined by PCA on the whole-cell spectra

Journal Pre-proof

Declaration of interests

The authors declare that they have no known competing financial interests or personal relationships that could have appeared to influence the work reported in this paper.

The authors declare the following financial interests/personal relationships which may be considered as potential competing interests:

Journal Pre-proof